PHYSICAL REVIEW D VOLUME 40, NUMBER 3 1 AUGUST 1989

$W^{\pm}H^{\mp}$ production at hadron colliders

D. A. Dicus
Center for Particle Theory, University of Texas, Austin, Texas 78712

J. L. Hewett
Department of Physics, University of Wisconsin, Madison, Wisconsin 53706

C. Kao
Center for Particle Theory, University of Texas, Austin, Texas 78712

T. G. Rizzo
Department of Physics, University of Wisconsin, Madison, Wisconsin 53706
and Ames Laboratory and Department of Physis, Iowa State University, Ames, Iowa 50011
(Received 23 March 1989)

We have examined the production of a charged Higgs boson in association with a W boson at high-energy hadron colliders, i.e., $pp \to W^{\pm}H^{\mp}+X$, and find that the production rates can be large. The various subprocesses which contribute to this mechanism at the tree and one-loop levels are compared and we find that quark annihilation $b\bar{b}, t\bar{t} \to W^{\pm}H^{\mp}$ is dominant. Production via gluon-gluon fusion, which proceeds through box and triangle diagrams, is also found to yield a significant contribution. We also compare our results with those obtained in rank-5 E_6 models for this process.

One of the least understood aspects of the standard model (SM) is the Higgs sector which is responsible for spontaneous symmetry breaking (SSB) and the generation of masses for the fermions and gauge bosons. Whereas the SM leads to a single Higgs scalar after SSB, extensions of the SM can lead to additional physical spin-zero fields. In the two-Higgs-doublet extension, after SSB, there remains a pair of singly charged Higgs bosons, two neutral scalars, and a neutral pseudoscalar. Clearly, the detection of the SM Higgs boson, or the Higgs fields of any extended model, will greatly clarify our knowledge of this mysterious sector of electroweak gauge theories.

Future colliders, such as the Superconducting Super Collider (SSC) and the CERN Large Hadron Collider (LHC) are being designed in order to explore the nature of the Higgs sector. Even at these high-energy colliders the production rate for Higgs bosons of all kinds is usually small and signatures are not always easily detected even when they are produced. Although the production rates for both neutral and charged Higgs bosons are comparable at these high-energy hadron colliders, the neutral Higgs boson is much easier to identify. This is due to the fact that the neutral Higgs boson has a more spectacular signature since it may decay to gauge-boson pairs, while the charged Higgs boson decays dominantly into heavy-fermion pairs. One process which may be used to search for the charged Higgs boson which seems promising is the production of a charged Higgs boson in association with a W gauge boson: $pp \to W^{\pm}H^{\mp}+X$. The subsequent decays of the W would help identify the process as one to study for the presence of a charged Higgs boson. In this paper we examine this reaction and the various subprocesses which contribute to it in the two-Higgs-doublet extension of the SM. As will be discussed below, the general two-Higgs-doublet model contains too many independent parameters to analyze in a straightforward manner. Therefore, we will limit our discussion to the subset of models which satisfy the mass and mixing-angle relationships of the minimal supersymmetric model when calculating loop-order contributions to $W^{\pm}H^{\mp}$ production. $W^{\pm}H^{\mp}$ production may also occur in superstring-inspired E_6 theories due to the nonvanishing of the

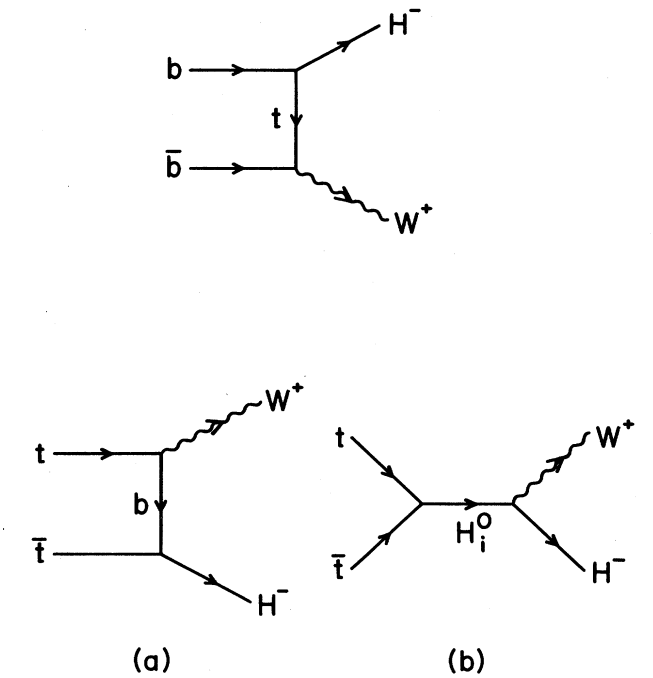

FIG. 1. Tree-level Feynman diagrams contributing to the $b\bar{b}, t\bar{t} \to W^{+}H^{-}$ process.

$WH(Z,Z')$ vertex in these models.

Let us now turn to the various mechanisms which contribute to $W^{\pm}H^{\mp}$ production. At the tree level the relevant subprocesses are $b\bar{b}\to W^{\pm}H^{\mp}$ and $t\bar{t}\to W^{\pm}H^{\mp}$ with the corresponding diagrams shown in Figs. 1(a) and 1(b). For the $b\bar{b}$ process we have the cross section ($z=\cos\theta$)

$$\frac{d\hat{\sigma}(b\bar{b}\to W^+H^-)}{dz}=\frac{\pi\alpha^2}{96x_W^2}\frac{m_t^4}{M_W^2\hat{s}}\frac{\cot^2\beta}{(\hat{t}-m_t^2)^2}\times\left[\hat{s}+\frac{(\hat{u}-M_W^2)(\hat{t}-M_W^2)}{M_W^2}\right]\times\left[\left[1-\frac{M_W^2+m_H^2}{\hat{s}}\right]^2-\frac{4M_W^2m_H^2}{\hat{s}^2}\right]^{1/2},\tag{1}$$

where $\alpha^{-1}\simeq 128$, $x_W=\sin^2\theta_W\simeq 0.230$, $\tan\beta=v_2/v_1$, with v_i being the two doublet vacuum expectation values, and m_H is the charged-Higgs-boson mass. (For $b\bar{b}\to W^-H^+$, $\hat{t}\leftrightarrow\hat{u}$.) In writing this cross section we have employed the couplings of Gunion and Haber[1] and have neglected the b-quark mass as we will do in all of our calculations below. The corresponding expression for $t\bar{t}\to W^+H^-$ is more complicated since there are now non-negligible scalar and pseudoscalar-exchange contributions in the s channel which are shown in Fig. 1(b). We find the cross section in this case to be given by

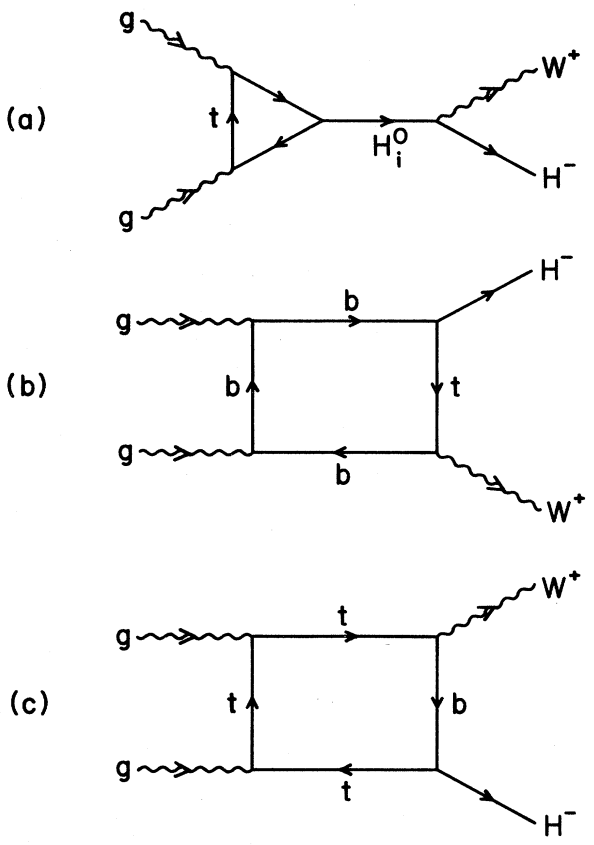

FIG. 2. One-loop box and triangle diagrams contributing to $gg\to W^+H^-$ production.

$$\frac{d\hat{\sigma}(t\bar{t}\to W^+H^-)}{dz}=\frac{\pi\alpha^2}{96x_W^2}\frac{m_t^2}{M_W^2\sqrt{\hat{s}}(\hat{s}-4m_t^2)^{1/2}}\left[\left[1-\frac{M_W^2+m_H^2}{\hat{s}}\right]^2-\frac{4M_W^2m_H^2}{\hat{s}^2}\right]^{1/2}\left[\cot^2\beta\left[\frac{T_1}{4\hat{t}^2}+\frac{T_4}{D_3^2}+\frac{T_5}{2\hat{t}D_3}\right]+\Sigma^2T_2+\frac{\cot\beta}{2\hat{t}}\Sigma T_3\right],\tag{2}$$

where $D_i\equiv\hat{s}-m_i^2$ with m_i ($i=1,2,3$) being the two ($i=1,2$) neutral scalar and the pseudoscalar ($i=3$) Higgs-boson masses and

$$\Sigma\equiv\frac{\sin^2\alpha\cot\beta-\frac{1}{2}\sin2\alpha}{D_1}+\frac{\cos^2\alpha\cot\beta+\frac{1}{2}\sin2\alpha}{D_2}\tag{3}$$

with α being the mixing angle between the two neutral Higgs scalars. The T_a ($a=1,\ldots,5$) are given by

$$T_1=4(\hat{t}+m_t^2-M_W^2)(m_H^2-\hat{t}-m_t^2)-4\hat{t}(\hat{s}-2m_t^2)+\frac{4}{M_W^2}(m_t^2+M_W^2-t)[(m_t^2-M_W^2)(m_H^2-\hat{t}-m_t^2)-\hat{t}(\hat{s}-2m_t^2)],$$

$$T_2=2(\hat{s}-4m_t^2)\left[-\hat{s}+\frac{1}{4M_W^2}(M_W^2-m_H^2+\hat{s})^2\right],$$

$$T_3=4[\hat{s}(\hat{t}+m_t^2-m_H^2)+2m_t^2(m_H^2-M_W^2)]+\frac{2}{M_W^2}(M_W^2-m_H^2+\hat{s})\times[-\hat{s}\hat{t}+m_t^2(2\hat{t}+m_H^2+M_W^2-2m_t^2)],\tag{4}$$

$$T_4=2\hat{s}\left[-\hat{s}+\frac{1}{4M_W^2}(M_W^2-m_H^2+\hat{s})^2\right],$$

$$T_5=4\hat{s}(\hat{t}+m_t^2-m_H^2)+\frac{2}{M_W^2}(M_W^2-m_H^2+\hat{s})[-\hat{s}\hat{t}+m_t^2(m_H^2-M_W^2)].$$

Again, the corresponding $t\bar{t}\to W^-H^+$ cross section can be obtained from the above by the substitution $\hat{t}\leftrightarrow\hat{u}$. These results hold for general two-doublet models in which a single Higgs doublet is responsible for giving mass to a fermion of a given electric charge.

At the one-loop level gluon-gluon fusion can make a significant contribution to $W^{\pm}H^{\mp}$ production via box and triangle diagrams (as shown in Fig. 2) containing virtual b and t quarks. As in Ref. 2 our method of calculating these loop diagrams is to make use of Veltman's code FORMFactor.[3] The triangle diagrams leading to the s-channel Higgs-boson-exchange contributions to $W^{\pm}H^{\mp}$ production can be readily evaluated by analytical methods, but the box diagrams cannot be so easily evaluated since they involve hundreds of Spence functions. The FORMFactor program calculates these Spence functions and combines them into various Feynman integrals. The resulting numerical program is then checked by replacing the polarization vector for one of the gluons by its four-momentum. Gauge invariance requires that this yields a vanishing result, which it does to great accuracy in most cases. Since it is the easiest way to also determine the interference between the box and triangle diagrams, FORMFactor has been used to evaluate the triangle diagram as well.

To proceed with our calculation, a large number of *a priori* unknown parameters need to be supplied: α, β, m_i, m_H, and m_t. In order to reduce these to a more manageable set, as discussed above, we will assume that the relations between these parameters in the minimal version of the supersymmetric standard model[1] hold; hence β and m_H become the only free parameters (in addition to m_t). Thus we have

$$m_3^2=m_H^2-M_W^2 ,$$

$$m_{1,2}^2=\tfrac{1}{2}\{m_3^2+M_Z^2\pm[(m_3^2+M_Z^2)^2-4m_3^2M_Z^2\cos^2 2\beta]^{1/2}\} ,$$

$$\cos 2\alpha=-\cos 2\beta\left[\frac{m_3^2-M_Z^2}{m_1^2-M_Z^2}\right] , \tag{5}$$

$$\sin 2\alpha=-\sin 2\beta\left[\frac{m_1^2+m_2^2}{m_1^2-m_2^2}\right] ,$$

$$|\cos(\beta-\alpha)|=\left[\frac{m_2^2(M_Z^2-m_2^2)}{(m_1^2-m_2^2)(m_1^2+m_2^2-M_Z^2)}\right]^{1/2} .$$

These relations imply that $m_H>M_W$ and $m_2<M_Z<m_1$. Note that these relations imply that the denominators D_i in Eqs. (2) and (3) above never vanish. It is important to realize that these relations do not hold in a general two-doublet model.

Now that we can evaluate the differential cross sections, the corresponding total cross sections are obtained by integration after weighting by the appropriate set of parton distribution functions (we use set I of Duke and Owens[4] and for the heavy quarks, the code developed by Collins and Tung[4] with set I of Duke and Owens as input). For the gluon-fusion and quark-annihilation subprocesses we then have

$$\sigma=\int_{M_W+m_H}^{\sqrt{s}}\frac{2\mathcal{M}}{s}d\mathcal{M}\int_{-Y}^{Y}dy\left\{\begin{matrix} g(x_1,\mathcal{M}^2)g(x_2,\mathcal{M}^2) \\ q(x_1,\mathcal{M}^2)\bar{q}(x_2,\mathcal{M}^2)+q(x_2,\mathcal{M}^2)\bar{q}(x_1,\mathcal{M}^2)\end{matrix}\right\}\int_{-z_0}^{z_0}dz\left[\frac{d\hat{\sigma}}{dz}\right] . \tag{6}$$

Here $\mathcal{M}$ is the $W^{\pm}H^{\mp}$ invariant mass, Y is a rapidity cut (which we take to be 2.5), and we have defined

$$x_{1,2}=\frac{\mathcal{M}}{\sqrt{s}}e^{\pm y},\quad Z_0=\min[\beta^{-1}\tanh(Y-|y|),1] , \tag{7}$$

with

$$\beta=\left[\left[1-\frac{M_W^2+m_H^2}{\mathcal{M}^2}\right]^2-\frac{4M_W^2m_H^2}{\mathcal{M}^4}\right]^{1/2}\times\left[1+\frac{M_W^2-m_H^2}{\mathcal{M}^2}\right]^{-1} . \tag{8}$$

In our calculation of the triangle and box diagrams, we first note that both amplitudes have almost identical magnitudes but with opposite signs for all values of $\tan\beta$, m_t, and m_H. This relative sign between the box and triangle contributions is fixed by the requirement that the $t\bar{t}\to W^{\pm}H^{\mp}$ and $t\bar{t}\to H_i^0\to W^{\pm}H^{\mp}$ parts of the graphs satisfy unitarity at high energies. This cancellation is shown schematically in Fig. 3 at SSC energies ($\sqrt{s}=40$ TeV) for $m_t=100$ GeV and $\tan\beta=1.2$ as a function of m_H. This is somewhat disappointing since the relative minus sign produces destructive interference and an approximate order-of-magnitude decrease in the box plus triangle contribution to $W^{\pm}H^{\mp}$ production. This deli-

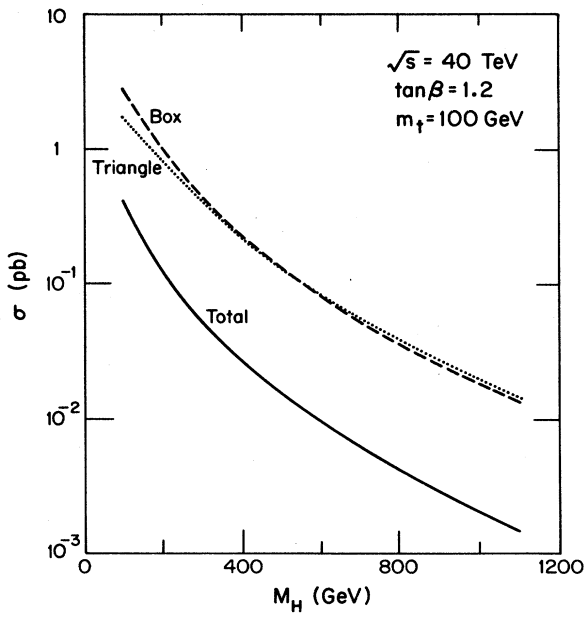

FIG. 3. A comparison of box and triangle diagram contributions and their sim to $W^{\pm}H^{\mp}$ production with $\sqrt{s}=40$ TeV, $\tan\beta=1.2$, and $m_t=100$ GeV as a function of the charged-Higgs-boson mass.

cate cancellation is, of course, due to the mixing and mass relationships in Eq. (5). In more general models, the sum of triangle and box diagram will be somewhat larger than what is presented here.

Figures 4 and 5 show the total production cross sections (summing over W^+H^- and W^-H^+) as a function of m_H at the SSC ($\sqrt{s}=40$ TeV) and the LHC ($\sqrt{s}=17$ TeV), respectively, for different tanβ values. The individual contributions from gluon-gluon fusion (gg) as well as $t\bar{t}$ and $b\bar{b}$ annihilation for different m_t values are shown. Note that for fixed m_H, as tanβ increases, σ is found to decrease. The rate for $W^{\pm}H^{\mp}$ production is comparable to that found earlier for ZH^0 production.[2] Also shown in these figures is the $W^{\pm}H^{\mp}$ production cross section in rank-5 E_6 models[5] via the s-channel exchange of a Z' boson[6] ($q\bar{q}\to Z,Z'\to W^{\pm}H^{\mp}$) for two different Z' mass values. The expression for the cross section for this process is given in Ref. 6 and the figures show that for fixed m_H this cross section increases with tanβ. This process probes the $W^{\pm}H^{\mp}(Z,Z')$ vertices

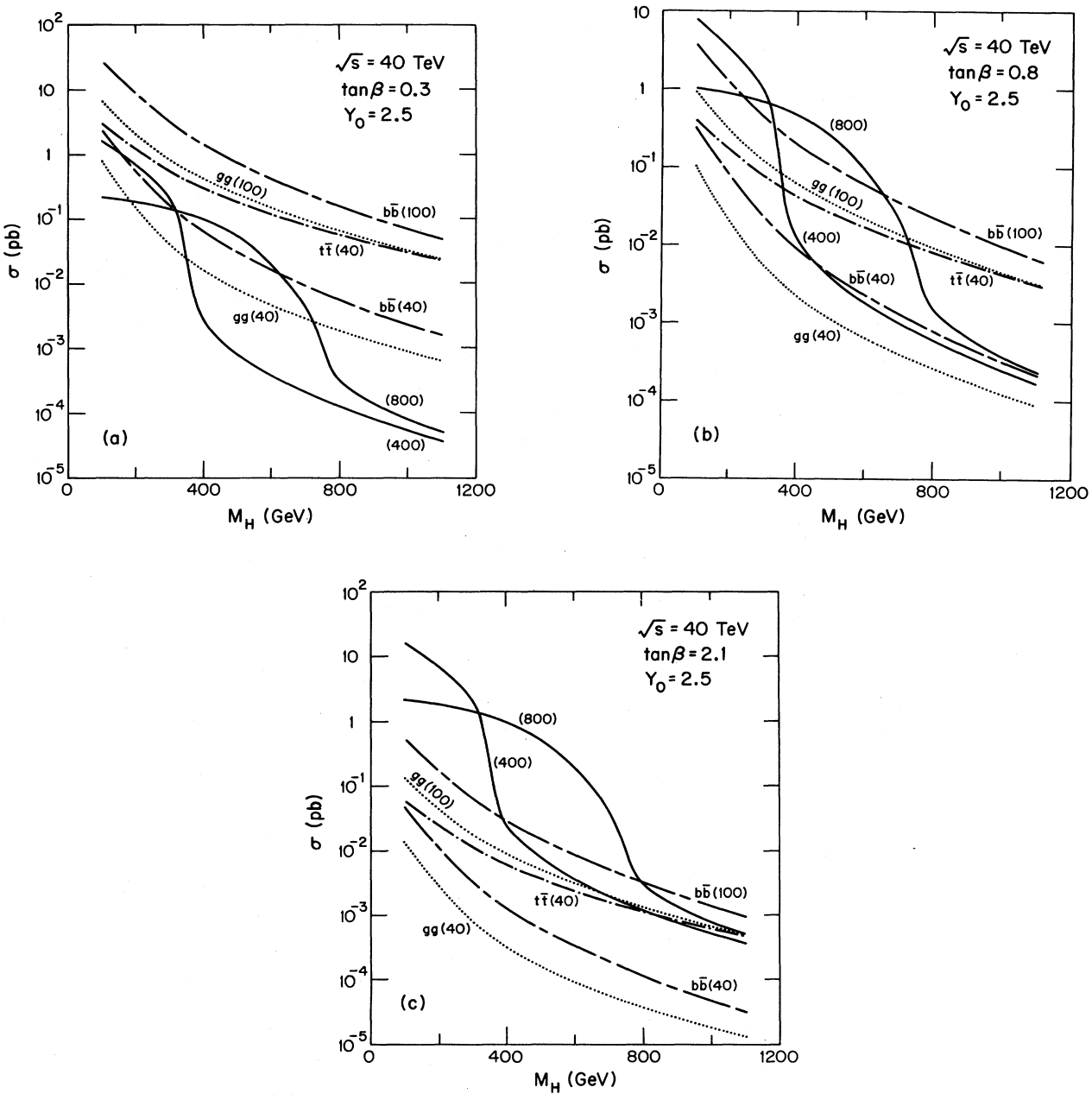

FIG. 4. Total cross section for $W^{\pm}H^{\mp}$ production as a function of the charged-Higgs-boson mass at the SSC ($\sqrt{s}=40$ TeV) with a $Y\leq 2.5$ rapidity cut, showing the m_t dependence of the various subprocesses for (a) tan$\beta=0.3$, (b) tan$\beta=0.8$, and (c) tan$\beta=2.1$. The rank-5 E_6 model prediction is also shown for two different Z' masses (400 and 800 GeV).

present in such models as well as the amount of Z-Z' mixing. For $\tan\beta=0.3$, the two-Higgs-doublet model prediction surpasses that of the E_6 process for all values of m_H. If $\tan\beta=0.8$ and lighter values of m_H are chosen, the E_6 process is dominant and for $\tan\beta=2.1$ it dominates for all but large values of m_H. It should be noted that the relative sizes of the two-Higgs-doublet and E_6 model predictions are somewhat sensitive to $\sqrt{s}$ with the ratio of the E_6 to the two-Higgs-doublet contributions being somewhat larger at the LHC.

The $t\bar{t}$ contribution is shown only for $m_t=40$ GeV

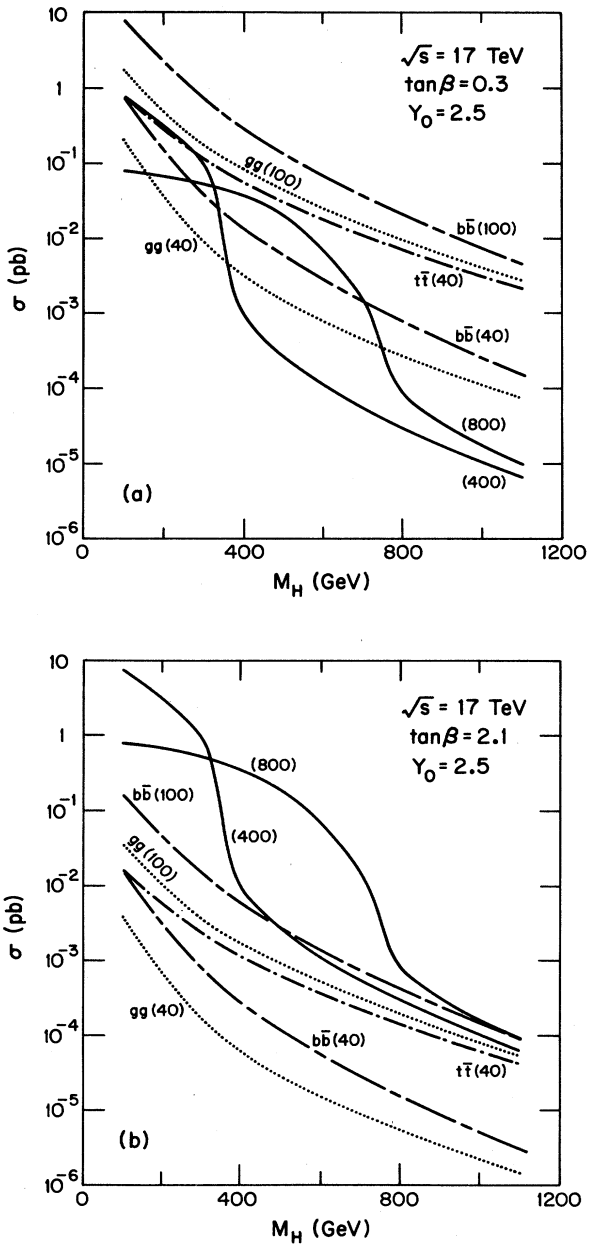

FIG. 5. Same as Fig. 4 but for the LHC ($\sqrt{s}=17$ TeV) with (a) $\tan\beta=0.3$ and (b) $\tan\beta=2.1$.

since a slight difficulty arises when $m_H>m_t>M_W$ (or $m_H<m_t<M_W$). In this mass regime, a pole develops in the t-channel, b-exchange graph where $t\to Wb$ and $\bar{t}b\to H$ (or $\bar{t}\to H\bar{b}$ and $\bar{b}t\to W$) are kinematically allowed. If m_b is taken to be nonzero then this can occur only for a range of values of $\hat{s}$ but these values are still within the physical region. This kinematic pole is not unique to this process. For example, if $m_t>M_W$, it would occur in $t\bar{b}\to W^+Z$ for $\hat{s}>m_t^2(M_Z^2-M_W^2+m_t^2)/(m_t^2-M_W^2)$. In order to remove this pole the production of the initial $t\bar{t}$ must be considered (i.e., the process $gg\to t\bar{t}t\bar{t}\to t\bar{t}W^{\pm}H^{\mp}$) and care must be taken to avoid double counting. It should also be noted that in the SM, a calculation[7] of $t\bar{t}\to H^0$, $gt\to H^0$, $g\bar{t}\to\bar{t}H^0$, and $gg\to t\bar{t}H^0$, using the couplings of Ref. 1, found that $t\bar{t}\to H^0$, for $m_t=40$ GeV, overestimated the "true" cross section by a factor of approximately 2.5. Thus our values for $t\bar{t}$ may be slightly too large. This also requires a calculation of $gg\to t\bar{t}W^{\pm}H^{\mp}$; these calculations are now in progress.[8]

To get an idea of rates let us focus our attention on a reasonably light charged-Higgs-boson mass $m_H\simeq 300$ GeV. For $\tan\beta=0.3$ (0.8, 2.1) and $m_t=100$ GeV, the production cross section at the SSC in the two-Higgs-doublet model is found to be $\sigma\simeq 4$ (0.5, 0.1) pb whereas in the E_6 rank-5 model we find $\sigma=0.2$ (0.7, 1.5) pb. We note that for a *neutral*-Higgs-boson mass of 300 GeV, the ZH^0 (where H^0 is the SM Higgs boson) production cross section[2] is 0.25 pb if $m_t=100$ GeV. In the ZH^0 case, a clean signature comes from $Z\to l^+l^-$ and $H^0\to W^+W^-\to l^+l^-\not{p}_T$ (or $H^0\to t\bar{t}\to W^+W^-b\bar{b}\to l^+l^-\not{p}_T+$soft jets) so that with well-identified τ's and an integrated luminosity of 10^4 pb^{-1}/yr we would expect 25 events/yr at the SSC. In the case of interest here, the cleanest signature is given by $H^+\to t\bar{b}\to W^+\bar{b}(+\text{soft } b)\to l^+l^-+\text{jets}+\not{p}_T$ with the associated W^- decaying leptonically: $W^-\to l^-\not{p}_T$. Folding in branching reactions and taking the same luminosity as above yields 480 (60, 13) events/yr at the SSC with $\tan\beta=0.3$ (0.8, 2.1) in the two-Higgs-doublet model. [The corresponding event rates in the rank-5 E_6 model are 24 (84, 180)/year.] Assuming the W^- in one hemisphere is well identified, the dominant background to this process arises from W^- production in association with two heavy-quark jets and may be removable by transverse mass cuts that identify the H^+ peak on the side opposite the W^- if enough statistics can be obtained.

To summarize, we have examined, in the context of the two-Higgs-doublet model, the production of charged Higgs bosons in association with W gauge bosons at the SSC and LHC via $pp\to W^{\pm}H^{\mp}+X$. The calculation involved several subprocesses both at the tree and one-loop levels and a large number of *a priori* unknown parameters. Use of the supersymmetric SM relations reduced the number of unknowns to three: m_t, M_H, and $\tan\beta$. For reasonable values of these parameters, we find cross sections which lead to significant signal rates at the SSC and LHC with the SSC producing the larger rates by a factor of 4–10 if identical luminosities are assumed. We also compared our results with those coming from rank-5

E_6 superstring-inspired models, which also can lead to $W^{\pm}H^{\mp}$ final states. The observation of $W^{\pm}H^{\mp}$ production may lead to a further understanding of the Higgs sector and SSB in general.

The authors would like to thank V. Barger, X. Tata, S. Willenbrock, and D. Zeppenfeld for helpful discussions. Computing resources for this work were provided by the University of Texas System Center for High Performance Computing. C.K. would like to acknowledge the Graduate School of the University of Texas at Austin for financial support. This work was supported in part by the U.S. Department of Energy under Contracts Nos. DE-FG05-ER8540200, DE-AC02-76ER00881, and W-7405-Eng-82 as well as the University of Wisconsin Research Committee with funds granted by the Wisconsin Alumni Research Foundation. T.G.R. would like to thank the Phenomenology Institute at the University of Wisconsin for its hospitality.

[1]J. F. Gunion and H. E. Haber, Nucl. Phys. **B272**, 1 (1986); **B278**, 449 (1986).

[2]D. A. Dicus, C. Kao, and W. W. Repko, Phys. Rev. D **36**, 1570 (1987); D. A. Dicus and S. Willenbrock, *ibid.* **37**, 1801 (1988); D. A. Dicus, *ibid.* **38**, 394 (1988); D. A. Dicus and C. Kao, *ibid.* **38**, 1008 (1988); D. A. Dicus, C. Kao, and S. S. D. Willenbrock, Phys. Lett. B **203**, 457 (1988).

[3]G. Passarino and M. Veltman, Nucl. Phys. **B160**, 151 (1979).

[4]D. Duke and J. Owens, Phys. Rev. D **30**, 49 (1984): J. C. Collins and W.-K. Tung, Nucl. Phys. **B278**, 934 (1986).

[5]J. L. Hewett and T. G. Rizzo, Phys. Rep. (to be published).

[6]T. G. Rizzo, Phys. Rev. D **39**, 728 (1989).

[7]D. A. Dicus and S. Willenbrock, Phys. Rev. D **39**, 751 (1989).

[8]D. A. Dicus *et al.* (in preparation).